Specific in vivo phosphorylation sites determine the assembly dynamics of vimentin intermediate filaments

John E. Eriksson[1,2,*], Tao He[2,3,4,‡], Amy V. Trejo-Skalli[5,‡], Ann-Sofi Härmälä-Braskén[2,3], Jukka Hellman[2], Ying-Hao Chou[5] and Robert D. Goldman[5]

[1]Department of Biology, Laboratory of Animal Physiology, University of Turku, Science Building 1, FIN-20014 Turku, Finland
[2]Turku Centre for Biotechnology, University of Turku and Åbo Akademi University, POB 123, FIN-20521 Turku, Finland
[3]Department of Biochemistry, Åbo Akademi University, FIN-20521 Turku, Finland
[4]Turku Graduate School of Biomedical Sciences, Kiinanmyllynkatu 13, FIN-20520, Turku, Finland
[5]Department of Cell, Molecular, and Structural Biology, Northwestern University Medical School, 303 E. Chicago Avenue, Chicago, IL-60611-3008, USA

‡These authors contributed equally to this work
*Author for correspondence (e-mail: john.eriksson@utu.fi)

Accepted 29 September 2003
Journal of Cell Science 117, 919-932 Published by The Company of Biologists 2004
doi:10.1242/jcs.00906

Summary

Intermediate filaments (IFs) continuously exchange between a small, depolymerized fraction of IF protein and fully polymerized IFs. To elucidate the possible role of phosphorylation in regulating this equilibrium, we disrupted the exchange of phosphate groups by specific inhibition of dephosphorylation and by specific phosphorylation and site-directed mutagenesis of two of the major in vivo phosphorylation sites determined in this study. Inhibition of type-1 (PP1) and type-2A (PP2A) protein phosphatases in BHK-21 fibroblasts with calyculin-A, induced rapid vimentin phosphorylation in concert with disassembly of the IF polymers into soluble tetrameric vimentin oligomers. This oligomeric composition corresponded to the oligopeptides released by cAMP-dependent kinase (PKA) following in vitro phosphorylation. Characterization of the ^{32}P-labeled vimentin phosphopeptides, demonstrated Ser-4, Ser-6, Ser-7, Ser-8, Ser-9, Ser-38, Ser-41, Ser-71, Ser-72, Ser-418, Ser-429, Thr-456, and Ser-457 as significant in vivo phosphorylation sites. A number of the interphase-specific high turnover sites were shown to be in vitro phosphorylation sites for PKA and protein kinase C (PKC). The effect of presence or absence of phosphate groups on individual subunits was followed in vivo by microinjecting PKA-phosphorylated (primarily S38 and S72) and mutant vimentin (S38:A, S72:A), respectively. The PKA-phosphorylated vimentin showed a clearly decelerated filament formation in vivo, whereas obstruction of phosphorylation at these sites by site-directed mutagenesis had no significant effect on the incorporation rates of subunits into assembled polymers. Taken together, our results suggest that elevated phosphorylation regulates IF assembly in vivo by changing the equilibrium constant of subunit exchange towards a higher off-rate.

Key words: Phosphorylation, Signaling, Intermediate filaments, Cytoskeleton, Dynamics

Introduction

Intermediate filaments (IFs) are composed of several classes of proteins that show a significant degree of diversity with respect to their sequences, expression patterns, and abundance in various tissues (Chou et al., 1996; Fuchs and Cleveland, 1998; Goldman et al., 1999; Omary and Ku, 1997; Skalli et al., 1992). Based on current knowledge, a main function of these proteins is to provide protection against various mechanical and possibly other types of stresses. Furthermore, IFs are involved in maintaining cell shape and providing a flexible scaffold, which maintains structural integrity and organization in the cytoplasm, organelles, and other cytoskeletal components (Chou et al., 1997; Fuchs and Cleveland, 1998; Omary and Ku, 1997).

A common feature of all these proteins is a coiled-coiled alpha-helical domain, which favors the formation of highly stable polymers. One way to affect the polymer stability and structure is phosphorylation of the constituent proteins. In fact, it seems that phosphorylation has a major role in regulating the structure and assembly of these proteins (Eriksson et al., 1992b; Inagaki, 1996; Ku et al., 1996). Recent studies have suggested that IF phosphorylation may also have other important functions, including regulating the connections of IFs with IF-associated proteins, the mediation of tissue-specific structural functions (Foisner et al., 1991; Ku et al., 1996; Liao and Omary, 1996) and in the regulation of IF structure and function by stress-activated kinases (Caulin et al., 2000; Feng et al., 1999; Giasson and Mushynski, 1996). Other studies have provided evidence that IFs are involved in regulating signaling and that this regulation in turn is controlled by phosphorylation. For example, it has been suggested that the phosphorylation-dependent assembly-disassembly equilibrium of vimentin IFs would regulate the activation state and targeting of RhoA-binding kinase α (Goto et al., 1998; Sin et al., 1998). In a similar fashion, keratins 8 and 18 have been shown to be associated with the attenuation of the tumor necrosis factor mediated signaling pathway (Caulin et al., 2000; Inada, 2001). Furthermore, phosphorylation regulates

the association of keratin 8/18 (Ku et al., 1998) and vimentin with 14-3-3 (Tzivion et al., 2000), a major regulator of many different signaling proteins (Aitken, 1996). It was also recently shown that the Raf-1 is associated with vimentin, and thereby may regulate the structure of vimentin filaments (Janosch et al., 2000).

IF proteins are good substrates for a number of kinases in vitro. These include the mitosis-specific p34cdc2 kinase [also established as a vimentin in vivo kinase (Chou et al., 1990; Chou et al., 1991)], as well as many different stimulus-specific kinases, for example, the various isoforms of PKC (Geisler et al., 1989), PKA (Ando et al., 1996), Ca/calmodulin-dependent kinase II (CAMK) (Ando et al., 1991; Tsujimura et al., 1994), RhoA-binding kinase α (Sin et al., 1998), c-Jun N-terminal kinase (Giasson and Mushynski, 1996; He et al., 2002), p21-activated kinase (Goto et al., 2002) and p38 kinase (Eriksson et al., 1992b; Feng et al., 1999; Inagaki, 1996; Ku et al., 1996).

There is a high constitutive protein phosphatase (PP) activity observed to be associated with IFs, suggesting that there is a high phosphate turnover on these proteins (Eriksson et al., 1992a). This activity appears to be related to two types of interphase-specific phosphorylation. One type renders a constitutive constant phosphorylation, usually with a low phosphate to protein stoichiometry, which may be temporarily elevated, depending on growth conditions, state of differentiation, etc. The other type of phosphorylation is related to a rather rapid constitutive turnover of phosphate on any given IF protein, as indicated by studies showing that PP inhibition leads to a very rapid increase in the phosphorylation of any given IF protein (Almazan et al., 1993; Eriksson et al., 1992a; Eriksson et al., 1992b; Lee et al., 1992; Ohta et al., 1992).

While different laboratories have reported that vimentin is a good in vitro substrate for a number of different kinases, with many different specific target sites (Eriksson et al., 1992b; Inagaki, 1996), it is not known how many of the identified in vitro sites could be relevant in vivo, with the exception of a few established in vivo sites. Furthermore, the biological role of the phosphorylation of such a large number of potential in vivo sites is far from clear. In the present study, we have attempted to establish all significant in vivo phosphorylation sites on vimentin. Furthermore, we wanted to determine the functional significance of the interphase-specific vimentin phosphorylation, with special reference to its role in the assembly/disassembly dynamics of vimentin (Miller et al., 1991; Prahlad et al., 1998; Vikstrom et al., 1989; Yoon et al., 1998). Our study identifies a large number of high turnover phosphorylation sites on vimentin, with PKA and PKC as potential regulatory kinases of several of these sites. The increased phosphorylation of these sites favors a depolymerized state, consisting of tetrameric subunits. We show that phosphorylation on two of the PKA-specific sites (Ser-38, Ser-72) leads to decelerated assembly kinetics of vimentin subunits in vivo, whereas obstruction of phosphorylation at these sites by site-directed mutagenesis has no significant effect on the incorporation rates of subunits into assembled polymers. Taken together, these results suggest that the dynamic exchange between the assembled and disassembled pool of vimentin in vivo is phosphorylation-dependent and occurs through an exchange of tetrameric subunits.

Materials and Methods

Cell culture and metabolic labeling

For metabolic labeling and treatment with the type-1 and type-2A protein phosphatase inhibitor calyculin-A (cl-A), BHK-21 cells were grown on plastic tissue culture Petri dishes (Falcon). Cells used for microinjection were grown on glass locator coverslips (Bellco Glass, Vineland, NJ). In either case, the culture medium used was Dulbecco's modified Eagle's medium (DMEM) supplemented with 10% (vol/vol) calf serum (Gibco-BRL). Metabolic labeling with [^{32}P]orthophosphate, treatment with cl-A and phosphopeptide mapping were carried as previously described (Chou et al., 1990; Eriksson et al., 1992a; Eriksson et al., 1998). For determination of in vivo phosphorylation sites, BHK-21 cells on four 100×20mm Petri dishes were preincubated for 4 hours with 0.5 mCi/ml [^{32}P]orthophosphate in phosphate-free DMEM with 10% fetal calf serum (approximate final phosphate concentration 0.1 mM). This preincubation time was found to saturate the cellular ATP pools. The cells were washed once with ice-cold PBS and lysed in Laemmli sample buffer (Laemmli, 1970). The in vivo labeled vimentin was separated by preparative SDS-PAGE, first on a 7.5% PAGE gel containing 6 M urea. The vimentin bands were then electroeluted and the vimentin was further purified by SDS-PAGE (7.5% acrylamide). The isolated protein could be seen as a single band on a gel stained with SYPRO Orange (Molecular Probes, Eugene, OR). The isolated vimentin was then subjected to tryptic digestion as previously described (Eriksson et al., 1992a; Eriksson et al., 1998) by using sequencing grade trypsin in a 5:1 molar ratio of vimentin:trypsin. For double labeling with ^{32}P and ^{35}S, BHK cells were preincubated with met/cys-free RPMI (Sigma) for 1 hour, followed by labeling with 250 μCi/ml ^{35}S (ICN) for 20 hours. The medium was afterwards changed to phosphate-free DMEM for 1 hour and labeled with ^{32}P (Amersham) as described above. Labeled cells were treated with 50 nM cl-A for 30 minutes. The cells were lysed in buffer containing 120 mM NaCl, 5 mM EGTA, 20 mM Hepes, 10 mM pyrophosphate, 0.5% Triton X-100, 50 nM cl-A, 1 mM phenylmethylsulfonyl fluoride and 10 μg/ml leupeptin/antipain/pepstatin, and centrifuged at 10,000 ***g*** for 5 minutes. The pellet containing the filament polymers was collected while the supernatant was further centrifuged at 200,000 ***g*** for 30 minutes to separate the fragmented filaments and the soluble subunits. Samples were run on SDS-PAGE and the autoradiography was carried out with and without four layers of aluminum foil between the gel and the film. The difference represented the signal from the ^{35}S labeling, which we used to calculate the specific amount of vimentin present in the samples.

Assays of vimentin subunit composition

Cells were incubated for 30 minutes in the presence of 50 nM cl-A. This treatment is sufficient to depolymerize at least 50% of the total vimentin pool. The cells were then lysed in a buffer containing 1% Triton X-100, 120 mM NaCl, 10 mM sodium pyrophosphate, 1 mM phenylmethyl sulfonylfluoride, 1 μg/ml aprotinin, and 10 μg/ml leupeptin and antipain, respectively. Cells were then centrifuged for 5 minutes at 10,000 ***g***, and the pellet (fraction 1) and part of the supernatant proteins (fraction 2) were denatured by boiling in Laemmli sample buffer. The remaining part of the supernatant was centrifuged at 200,000 ***g*** for 30 minutes and the supernatant proteins (fraction 3) were denatured by boiling in Laemmli sample buffer. The resultant proteins from these separations were categorized as follows: fraction 1: IF polymers; fraction 2: a mixture of fragmented IFs and solubilized subunits; and fraction 3: soluble subunits. The increase in the pool of fragmented and solubilized vimentin was assayed by western blotting. To determine the vimentin subunit composition, the vimentin in fraction 3 was crosslinked by incubating subsamples of the fraction for 10 minutes at room temperatures with increasing concentrations of glutaraldehyde as

described previously (Sistonen et al., 1994). The in vivo subunit composition was compared to that obtained by phosphorylating bacterially expressed human vimentin (see below) with protein kinase A (PKA). Purified human vimentin (1 mg/ml) was incubated for 30 minutes in the presence of activated PKA catalytic subunit (Sigma) in a buffer containing 20 mM Hepes, 60 mM NaCl, 2 mM $MgCl_2$, 5 mM EGTA and 100 μM ATP. In this buffer, vimentin is completely polymerized. Upon phosphorylation with PKA ~60-80% of the filaments are depolymerized into soluble subunits. The solubilized vimentin was isolated by centrifugation for 30 minutes at 200,000 ***g*** and the subunit composition was determined by SDS-PAGE after crosslinking, as described above.

Phosphopeptide mapping and in vitro phosphorylation

Purified human vimentin (1 mg/ml) was incubated for 30 minutes in the presence of activated PKA in a buffer containing 20 mM Hepes, 60 mM NaCl, 2 mM $MgCl_2$, 5 mM EGTA and 100 μM ATP. Protein kinase C (recombinant human PKCα; Calbiochem) phosphorylation was performed in the presence of Ca^{2+}, phosphatidylserine and diacylglycerol, according to the manufacturer's recommendations. Calcium/calmoduline-dependent kinase (CaMK) was kindly provided by Prof. Howard Schulman. Recombinant CaMKII-α (42 ng) was incubated with 25 μg recombinant vimentin and 60 U calmodulin (Sigma) in 100 μl CaMK reaction buffer, as described previously (Holmberg et al., 2001). Phosphorylation with p37 kinase (p37) and cdc2 kinase (cdc2 K) were performed exactly as previously described (Chou et al., 1990; Chou et al., 1991). Phosphatase treatment of PKA-phosphorylated bacterially expressed human vimentin was performed by incubation of phosphorylated vimentin with recombinant, α-isoform rabbit muscle protein phosphatase 1 (Calbiochem) at a concentration of 1 Unit/15 μg vimentin in a buffer containing 20 mM Hepes (pH 7.2), 1 mM $MgCl_2$, 30 mM β-mercaptoethanol, 10% glycerol and 1 mM $MnCl_2$, for 20 minutes at 30°C.

One-dimensional electrophoretic analysis of in vitro PKA-phosphorylated and phosphatase-treated vimentin was performed with 7.5% acrylamide SDS-PAGE (Laemmli, 1970), followed by autoradiography using Kodak X-Omat film. Radioactive phosphate content of vimentin contained within gel slices was determined using a scintillation counter.

Tryptic cleavage of ^{32}P-labeled vimentin phosphorylated either in vitro or in vivo, followed by two-dimensional phosphopeptide mapping, was carried out as previously detailed (Chou et al., 1990; Eriksson et al., 1992a; Skalli et al., 1992). Autoradiography was performed as described above.

Determination of the specific phosphorylation sites on vimentin

BHK cells were preincubated for 4 hours with 0.5 mCi/ml $^{32}PO_4$ in DMEM containing 0.1 mM phosphate. Cells were then washed with PBS, and lysed in Laemmli sample buffer. In vivo labeled vimentin was purified according to a two-step preparative SDS-PAGE protocol as follows. The labeled vimentin was first separated on a large 30 cm SDS-PAGE gel, the radiolabeled vimentin was excised and the protein was electroeluted. The electroeluted material was separated on a 30 cm SDS-PAGE gel containing 6 M urea, which quantitatively separated vimentin from desmin. The gel was fixed with 50% methanol/water, the vimentin band was excised according to the autoradiographic pattern, and the whole amount of vimentin (approximately 100 μg) was digested in the gel overnight at 37°C with 10 μg sequencing grade trypsin (Boehringer Mannheim, Germany). The yielded peptides were dried with speed-vac and injected into an Aquapore RP-300 C-18 (Brownlee/Perkin-Elmer, Shelton, Connecticut) microbore column (flow-rate 0.1 ml/ml, abs. 215 nm). The column was developed with elution buffers A (0.1% trifluoroacetic acid/water) and B (80% acetonitrile, 0.08% trifluoroacetic acid/water), using the following gradient: 0-15 minutes 0% B, 15-85 minutes 40% B, 85-100 minutes 60% B, 100-110 minutes 100% B. Fractions were collected at 1-minute intervals and a small aliquot of each fraction was spotted on filter paper. The radiolabeled fractions was collected based on the phosphorimager pattern of the membrane. The radiolabeled fractions were further purified by using an Aquapore OD-300 C8 (Brownlee/Perkin-Elmer) microbore column (flowrate 0.1 ml/min) with the same buffer system as in the first separation: 0-10 minutes 0% B, 10-25 minutes 30% B, 25-60 minutes 50% B, 60-90 minutes 100% B.

Manual Edman degradation was performed essentially as described previously (Eriksson et al., 1998). NH_2-terminal amino acid sequence analyses of the tryptic peptides were performed with an Applied Biosystems model 477A protein sequencer equipped with an Applied Biosystems model 120A on-line phenylthiohydantoin amino acid analyzer. The samples were applied to a polybrene-coated and precycled glass fiber filter. Standard cycle parameters were employed for a desired number of cycles.

Site-directed mutagenesis and bacterial expression of vimentin

Human vimentin cDNA, engineered with a myc-tag cassette attached to the C terminus at a *Sph*I site located at the end of the vimentin coding sequence, was expressed in *E. coli* and purified exactly as was previously described (Chou et al., 1996). The vimentin (HBEV) was stored at –80°C in aliquots at a concentration of 1 mg/ml in 5 mM sodium phosphate (pH 7.4) microinjection buffer.

A mutated version of the human vimentin was made by substituting the major sites of PKA phosphorylation, Ser-38 and Ser-72 with alanine. This was accomplished by using human vimentin cDNA cloned into the M13 bacteriophage vector in the site-directed mutagenesis procedure described by Kunkel (Kunkel, 1985). This method makes use of a uracil containing single-stranded DNA template. Based on this, a double mutant S38:A/S72:A version of human vimentin cDNA was made using two primers: S38:A---T-CCACCCGCACCTACGCCCTGGGCGACGCG; and S72:A---GTGCGCCTGCGGAGC-GCCGTGCCCGGGGTG. Mutagenesis was confirmed using double-stranded DNA sequencing. A fragment of the human vimentin cDNA containing the two mutations was excised from the M13 double-stranded DNA using *Bam*HI and *Xho*I restriction enzymes (Gibco-BRL). This ~400 base pair fragment was cloned into the pET-7 vector by swapping the mutated fragment for the corresponding wild-type vimentin fragment, generating the S38:A/S72:A pET-7 myc-tagged human vimentin cDNA construct.

Microinjection, immunofluorescence and confocal microscopy

Myc-tagged vimentin was microinjected at 1 mg/ml in 5 mM sodium phosphate buffer pH 7.4, into BHK fibroblasts with the aid of a Zeiss inverted phase-contrast microscope fitted with a Narishige NT-88 hydraulic microinjector-micromanipulator (Vikstrom et al., 1989). At various time points following microinjection, cells were fixed with methanol for 5 minutes at –20°C. Indirect immunofluorescence was performed using undiluted, Tris-buffered (pH 8.0) culture supernatant containing monoclonal antibody 9E10 directed against the myc tag (American Type Culture Collection, Bethesda, MD). For double-labeling, a polyclonal antiserum directed against BHK vimentin was used (Yang et al., 1985), at a dilution of 1:20 in PBS. Secondary antibodies were: FITC-labeled donkey anti-mouse IgG and lissamine-rhodamine-labeled donkey anti-rabbit IgG (Jackson ImmunoResearch Laboratories), all of which were also diluted 1:20 in PBS. Recombinant vimentin was phosphorylated by PKA as described above. The reaction was stopped by addition of 8 M urea. The urea was dialyzed against 5 mM sodium phosphate buffer (pH 4). During this procedure, vimentin was renatured but PKA did not regain its activity. Microscopic observations were made using an LSM 410 confocal microscope (Carl Zeiss, Inc., Thornwood, NY) equipped

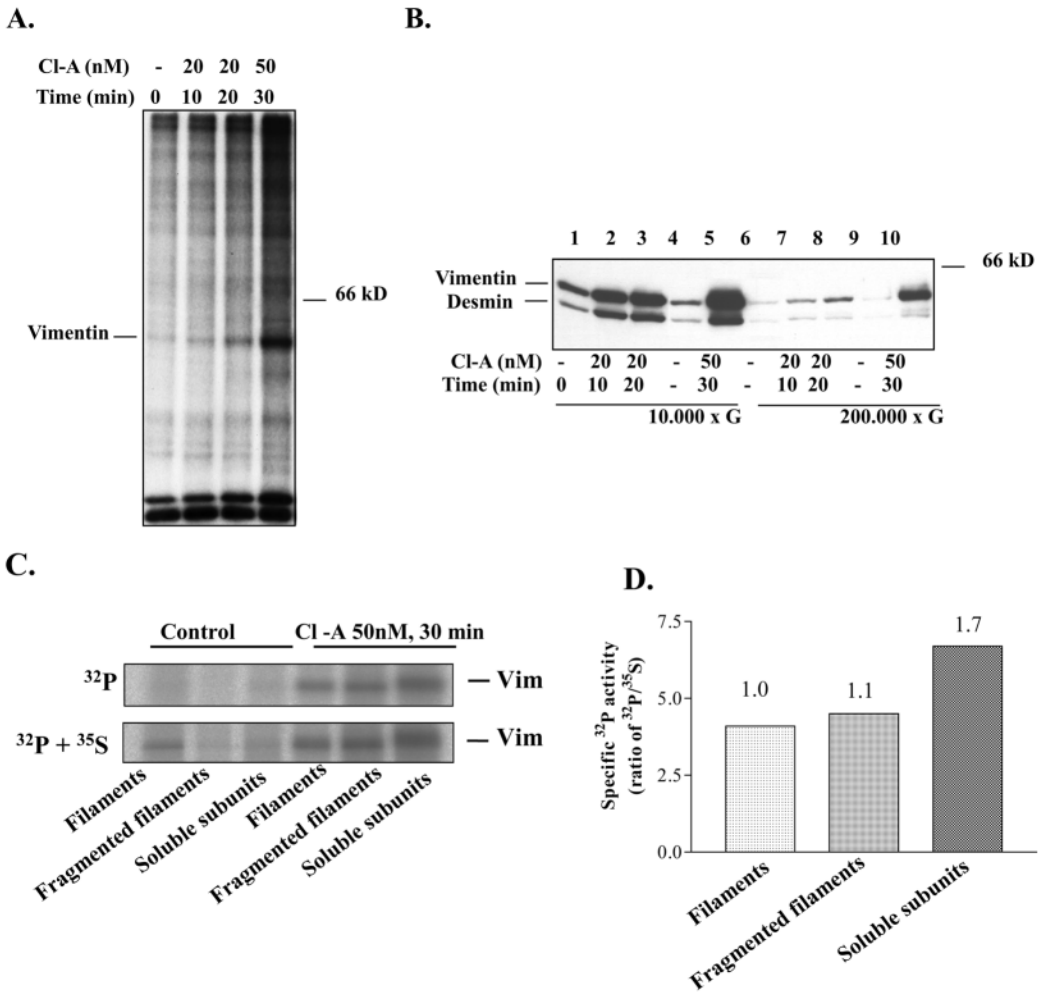

Fig. 1. Inhibition of vimentin dephosphorylation in vivo induces hyperphosphorylation and disassembly of vimentin polymers. (A) ^{32}P in vivo labeled BHK-21 cells were incubated without or with 20 nM of the protein phosphatase inhibitor cl-A for 10 and 20 minutes and with 50 nM cl-A for 30 minutes. The inhibition of constitutive vimentin phosphatase activities causes a dose and time-dependent elevation of vimentin phosphorylation, as shown in the autoradiography of the ^{32}P in vivo labeled proteins separated by 10% SDS-PAGE. (B) The phosphorylation causes a disassembly of the vimentin IF filaments, which is reflected by their increase in both the low and high speed centrifugation supernatants, as measured by western blotting of the respective supernatant fractions. While the IF pool in the low speed supernatant is primarily composed of both large filament fragments and soluble subunits, the high speed supernatant contains only truly soluble subunits. The vimentin levels are elevated both in the low and high speed supernatants but desmin concentrations are only elevated in the low speed supernatants. This implies that desmin is not disassembled under these conditions into soluble subunits but merely fragmented. This is consistent with the phosphorylation of desmin, which is not elevated by inhibition of dephosphorylation. (C) The specific phosphorylation (^{32}P labeling/protein units) of polymer-associated and depolymerized vimentin subunits was analyzed by double in vivo labeling with [^{32}P]orthophosphate and [^{35}S]methionine followed by phosphorimager analysis ($^{32}P + {}^{35}S$ is the signal collected from both isotopes on the gel; the ^{32}P signal was obtained by exposure through four layers of aluminum foil). The results indicate that phosphate incorporation takes place both on polymer-associated vimentin and on the dissociated subunits, as shown by (D) quantification of the same specific levels of ^{32}P per protein unit ($^{32}P/^{35}S$), with a certain preference for phosphate incorporation into the soluble subunits, as indicated by the ratios between the different protein pools, as compared to the filamentous pool (=1), shown above the bars.

with 100× oil immersion, 1.3 NA objective lens and an argon/krypton laser.

Results

Phosphatase inhibition induces hyperphosphorylation and disassembly of vimentin IFs in vivo

The availability of well characterized protein phosphatase inhibitors makes it possible to hyperphosphorylate IF proteins in vivo and to characterize their specific phosphorylation sites. To this end, we used the specific type-1 (PP1) and type-2A (PP2A) protein phosphatase inhibitor, calyculin-A (cl-A), at concentrations sufficient to significantly downregulate the cellular activities of these two major phosphatases (Eriksson et al., 1998; Li et al., 1993). Previous studies on BHK-21 cells have shown that short term treatment with cl-A under these conditions does not induce any signs of cytotoxicity or apoptosis, and the effects on IFs at 20 nM are reversible (Eriksson et al., 1992a). Protein phosphatase inhibition resulted in a rapid dose- and time-dependent elevation of the ^{32}P labeling of vimentin (Fig. 1A). Furthermore, this elevated phosphorylation resulted in a rapid disassembly of IF into pelletable and non-pelletable fractions (Fig. 1B). In order to elucidate possible differences in relative phosphate stoichiometry of the disassembled protein pool versus the assembled polymers, we performed metabolic double labeling of the BHK cells with [^{32}P]orthophosphate and [^{35}S]methionine. The specific ^{32}P activity was then determined as a ratio of $^{32}P/^{35}S$. Upon PP inhibition there was a marked increase in the specific labeling of both pelletable and non-pellatable fractions. The specific ^{32}P labeling was in the truly soluble subunit fraction, as compared to both filament-containing fractions, whereas the pelletable vimentin fractions (filaments and fragments) were labeled to the same extent (Fig.

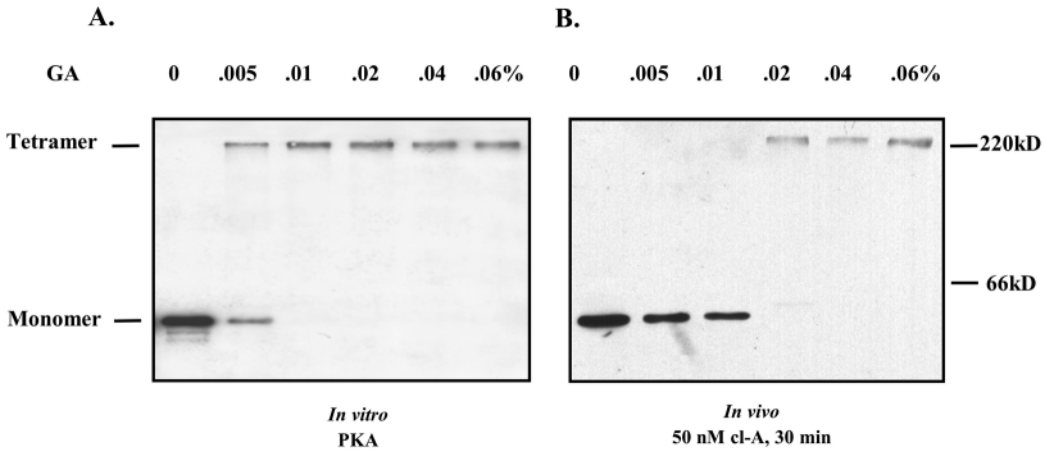

Fig. 2. Phosphorylation-induced disassembly of vimentin IFs in vitro and in vivo results in disassembled subunits with the same molecular mass categories. (A) Bacterially expressed human vimentin IF polymers were phosphorylated in vitro by PKA and the resultant disassembly of depolymerized subunits was assayed by glutaraldehyde crosslinking (GA; concentration range: 0-0.06%) of the vimentin supernatant fractions after 30 minutes centrifugation at 200,000 ***g***. (B) The in vitro disassembly of vimentin was compared to that in vivo, by incubating BHK-21 cells in the presence of 50 nM cl-A for 30 minutes. The cells were treated with 1% Triton X-100 and the particulate material was pelleted by centrifugation at 200,000 ***g*** for 30 minutes. The supernatants were then subjected to glutaraldehyde crosslinking (same concentration range as above) followed by immunoblottting. The results indicate that the phosphorylation-mediated release of vimentin subunits also occurs as tetramers in vivo.

1C,D). All fractions seemed to be phosphorylated on the same sites, as when phospopeptide mapping was performed on vimentin isolated from all three fractions, no obvious differences could be observed between the fractions in the phosphopeptide pattern (data not shown), indicating that their phosphorylation sites are the same.

The phosphorylation-induced disassembly of IF proteins results in the release of tetrameric subunits

In order to better understand the molecular dynamics of the phosphorylation-regulated equilibrium between assembled vimentin polymers and disassembled subunits, we determined the nature of the subunits released into the non-pelletable protein pool upon hyperphosphorylation of vimentin in vivo and in vitro. Cells were treated for 30 minutes with 50 nM cl-A and were lysed as described (see Material and Methods). Released subunits were crosslinked with increasing concentrations of glutaraldehyde (GA) after centrifugation of the cell extracts at 200,000 ***g***. The approximate molecular mass of the crosslinked vimentin subunits was 220 kDa, indicating that the bulk of the non-pelletable protein is tetrameric (Fig. 2B). This result was identical to the results obtained by the in vitro phosphorylation of vimentin with PKA (Fig. 2A). For comparison, the disassembled vimentin subunits were separated by centrifugation over sucrose gradients. In agreement with the crosslinking experiments, the non-pelletable vimentin appeared in fractions corresponding to the molecular masses of tetramers (data not shown).

Interphase-specific phosphorylation sites on vimentin and their potential kinases

We used phosphopeptide mapping of vimentin obtained from ^{32}P-labeled cells incubated in the presence and absence of cl-A to determine the in vivo phosphorylation sites on vimentin. Nine labeled phosphopeptides could be observed on maps obtained from untreated control cells, some of which are labeled so weakly that they are difficult to discern on control phosphopeptide maps (Fig. 3A). The same phosphopeptides, with significantly increased labeling, could be resolved on vimentin phosphopeptide maps obtained from phosphatase-inhibited cells (Fig. 3B). It was concluded that these phosphopeptides contained constitutive phosphate turnover sites on vimentin. Five of these sites (peptides 1, 2, 3, 4 and 7) contained ~80-90% of the increased labeling, indicating that these peptides contain the interphase-specific high phosphate turnover sites. The latter observation is in agreement with previous studies (Chou et al., 1990; Chou et al., 1991).

The phosphopeptide maps determined from in vivo preparations were compared with those obtained by phosphorylating vimentin in vitro with three interphase-specific (Fig. 3D-F) or two mitotic vimentin kinases (Fig. 3G,H). Two of the major interphase-specific phosphopeptides co-migrated with those generated by PKA (peptides 1 and 2, Fig. 3D). Phosphopeptides generated by PKC corresponded to minor sites on the in vivo maps (peptides 5, 6, and 8, Fig. 3E). As previously shown, the major phosphopeptides generated by the mitotic vimentin kinases p37 and cdc2 (Chou et al., 1990; Chou et al., 1991) corresponded to the major mitosis-specific peptides (Fig. 3G,H). However, the phosphopeptides generated by these kinases were also identified as minor spots on interphase maps, which could partly be due to the presence of a small percentage of unsynchronized cells in the cultures. Alternatively, these peptides may also contain minor interphase-specific sites. For example, PKC also generated a phosphopeptide corresponding to the cdc2-generated peptide 8. Furthermore, there are other proline-directed kinases that could generate a phosphopeptide pattern corresponding to that obtained with cdc2 kinase. The phosphopeptide revealed by CaMK runs close to peptide 2 on the peptide maps (Fig. 3F). However, when the identity of all of these peptides was checked by mixing the samples and by manual Edman degradation (data not shown), it turned out that peptide 2 is not the same peptide as the CaMK-generated peptide.

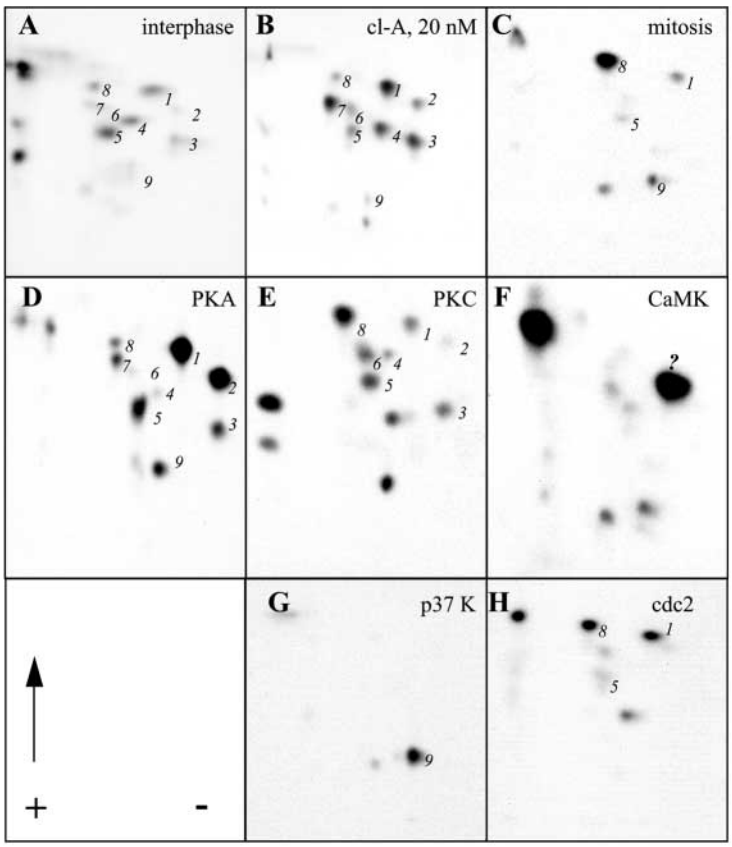

Fig. 3. Phosphopeptide mapping of the major interphase-specific in vivo phosphorylation sites on vimentin. (A) The relatively low level of ^{32}P-labeling of vimentin in interphase cells shown in Fig. 1, reflects constitutive phosphorylation on a few major sites, as indicated by the presence of a few more prominently labeled tryptic peptides (1, 4, 5, and 8) from vimentin isolated from untreated ^{32}P in vivo labeled BHK-21 cells. (B) When dephosphorylation is inhibited with 20 nM cl-A for 20 minutes, all (except peptide 8) of these constitutively labeled phosphopeptides displayed significant increases in labeling and, in addition, many new peptides (2, 3, 6, 7) showed marked elevations in ^{32}P labeling. These results indicate that there are some sites that maintain a certain level of constitutive phosphorylation and, in addition, some sites that are subjected to a high constitutive phosphate turnover. (C) The interphase-specific sites do not correspond to the mitosis-specific in vivo phosphorylation sites, as shown on a vimentin phosphopeptide map derived from in vivo labeled cells, blocked in metaphase by treatment with 2 μg/ml nocodazole for 3 hours. (D-H) The in vivo phosphopeptide maps were compared to those obtained by in vitro phosphorylation using a number of potential vimentin kinases. (D) PKA, (E) PKC, (F) CaMKII, (G) p37 K, and (H) cdc2 K, all resulted in characteristic phosphopeptide maps. Some of the major interphase-specific in vivo phosphopeptides showed a similar migration as the major phosphopeptides generated by PKA and PKC but not CaMK. The phosphopeptides generated by the mitotic kinases cdc2 K and p37 K did not correspond to any of the interphase-specific phosphopeptides but co-migrated with the major mitosis-specific phosphopeptides.

Determination of the specific in vivo phosphorylation sites on vimentin

For phosphopeptide identification, we used a rather high concentration (50 nM) of the PP inhibitor cl-A for the in vivo labeling of BHK-21 cells, to maximize the labeling of individual phosphorylation sites. This concentration was found to inhibit >95% PP1/PP2A activity (data not shown) without causing obvious cytotoxic effects, when used over short time periods. Highly purified ^{32}P-labeled vimentin was obtained by a preparative two-step SDS-PAGE protocol (see Materials and Methods). No other contaminating proteins could be detected by fluorometric analysis of 2D gels stained with Sypro Orange or by autoradiographic analyses of the gels (results not shown). Phosphorylated vimentin was then cleaved with trypsin and the resulting phosphopeptides were separated on a C-18 reversed phase microbore HPLC column. Seven major radiolabeled fractions (fractions a-g, Fig. 4A) were resolved. When these seven fractions were further purified on a C-8 reversed phased microbore HPLC column, eight radiolabeled peptides could be resolved, as fraction c yielded two peptides (peptides 3 and 4, Fig. 4B). At the second separation, the UV peaks corresponding to the labeled fractions indicated in all cases that the fractions were relatively well resolved into single phosphopeptides (Fig. 4B). The peptides were numbered based on their hydrophobicity and each peptide was sequenced, subjected to manual Edman degradation, and analyzed by MALD-TOF MS. Based on information obtained from the sequencing of the HPLC-isolated phosphopeptides (Table 1), from the molecular masses obtained on MALD-TOF mass spectrometry (data not shown), and from the results of manual Edman degradation (Table 1), the identity of the phosphopeptides and their phosphorylation sites could be assigned. In many cases, the mass spectrometric analysis yielded masses corresponding both to the native peptide and to the phosphorylated peptide, with one or two phosphate groups added, thus corroborating the phosphopeptide assignment (data not shown). In some cases, dehydroalanine was observed during the sequencing at a putative phosphoserine site, which

Fig. 4. Chromatographic separation of the major tryptic phosphopeptides from ^{32}P in vivo labeled vimentin. Four 20 cm plates of semi-confluent BHK-21 cells were preincubated for 4 hours with 0.5 mCi/ml [^{32}P]orthophosphate. In order to maximize the in vivo labeling, vimentin dephosphorylation was inhibited by addition of 50 nM cl-A to the cells. Vimentin was isolated by preparative SDS-PAGE as described in Materials and Methods and then subjected to tryptic cleavage. (A) The generated phosphopeptides were first isolated by reversed phase chromatography on a microbore C-18 column. The UV chromatogram (left panel) indicates the presence of a high number of tryptic peptides, among which seven ^{32}P labeled fractions were isolated (right panel; fractions a-g). (B) Peaks a-g obtained on the C18 chromatography were then separated a second time on a reversed phase microbore C-8 column, yielding one single purified peptide from fractions a, b and d-g, and two peptides from fraction c. The inserts show the elution profile of the ^{32}P label, which in all cases corresponded to a peak on the UV chromatogram. The isolated peptides were numbered according to their hydrophobicity on the C8 reversed phase HPLC. The obtained peaks were subjected to automatic sequencing and manual Edman degradation. Peptide masses were confirmed by mass-spectrometry (data not shown). The results are presented in Table 1.

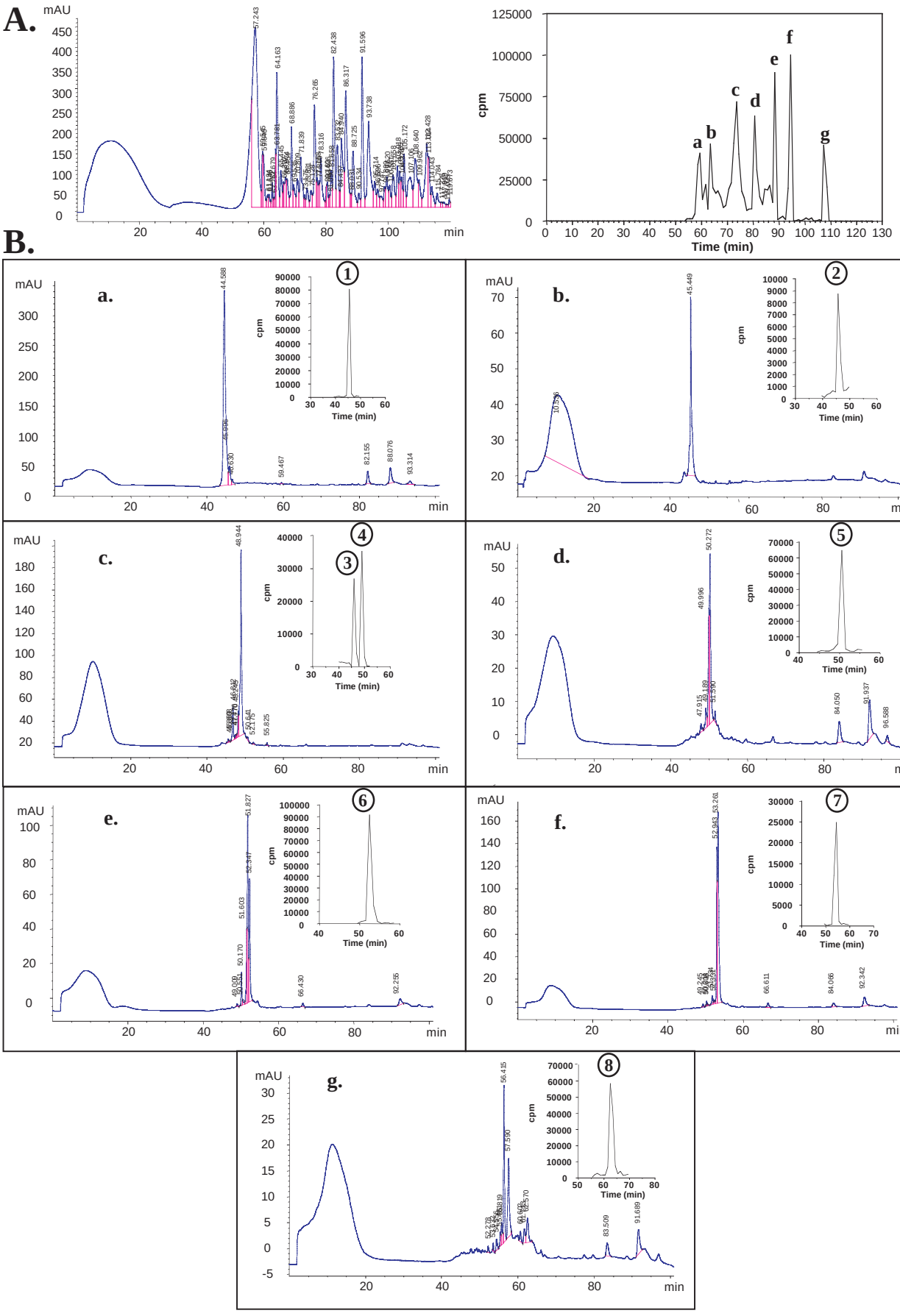
A.
mAU
min
cpm
Time (min)
a
b
c
d
e
f
g
B.
a.
b.
c.
d.
e.
f.
g.
1
2
3
4
5
6
7
8

Table 1. Information obtained on the phosphopeptides derived from in vivo labeled vimentin

Peptide number	Sequence obtained	% Label released on cycle number	Total number of cycles
1	**pS**VS**pS**SSYR	1 (10%), 4 (70%), D(<10%)	6
2	SV**pSpS**SSYR	3 (40%), 4 (50%), D (<10%)	6
3	LR**pSpS**MPGVR	3 (50%), 4 (40%), D (<10%)	6
4	DGQVINE**pTpS**QHHDDLE*	No release, D (>90%)	6
5	SLYSS**pS**PGGAYVTR	6 (90%), D (<10%)	6
6	TY**pS**LG**pS**AL	3 (60%), 6 (20%), D (<10%)	6
7	ETNLE**pS**LPLVDTHSK	6 (30%), D (>60%)	9
8	ISLPLPNFS**pS**LNLR	No release, D (>90%)	9

Phosphorylation sites (indicated in bold) on the basis of the results of the manual Edman degradation.

*The phosphorylation sites of peptide 4 to Thr-457 and Ser-458 were assigned based on the results of Chou et al. (Chou et al., 1996).

Peptides were numbered on the basis of increasing hydrophobicity on C8 HPLC. The sequence obtained for each isolated phosphopeptide is indicated together with the data obtained from the manual Edman degradation. The cycle in which release of label was observed during Edman degradation is shown. D refers to the crosslinked material remaining on the Sequelon membrane discs after completion of the Edman degradation cycles.

in these cases further supported the phosphorylation site assignment (during sequencing, dehydroalanine is spontaneously formed by β-elimination of phospho-Ser). Edman degradation was also performed on the TLC-based phosphopeptide maps (Fig. 3). Based on the obtained results fitted to the theoretical tryptic vimentin peptide sequences and combined with previous experience of the migration characteristics of previously isolated known vimentin phosphopeptides, the peptide identity of the spots on the vimentin phosphopeptides maps could be assigned with relatively high certainty (Table 2). Peptide 1 and 2 were from the far N-terminal region, representing two different phosphorylation variations of the stretch of the serines in that region. Further variations on this theme were observed among the phosphopeptides on the peptide maps (peptides 5,6,7; Table 2). These results imply that there is a very complex pattern of phosphorylation at the far N-terminal region, including Ser-4, 6, 7, 8 and 9, and that some vimentin molecules will contain a highly charged N terminus, with multiple phosphoserines. These sites were major targets for PKC (Fig. 3, Table 2). Peptide 3 contained two phosphoserines, i.e. Ser-71 and 72. These sites are major targets for PKA (Fig. 3, Table 2). Peptide 4 is from the C-terminal region, containing two phosphorylation sites, Thr-457 and Ser-458, that were assigned based on no release on the sixth Edman cycle and data from Chou et al. (Chou et al., 1996). These sites are targets for the mitotic p37 kinase (Chou et al., 1991; Chou et al., 1996). Peptide 5 was phosphorylated on Ser-55, which is the previously identified mitotic target for cdc2 (Chou et al., 1990). Peptide 6 contained two phosphorylation sites, Ser-38 and Ser-41. In addition to Ser-71 and 72, Ser-38 is a major target site for PKA (Fig. 3, Table 2). Peptide 7 contained one assigned phosphorylation site, Ser-429, from the C-terminal region (a significant amount of the label remained on the sequelon disc, so Thr-435 and/or Ser-437 could possibly be phosphorylation targets). Peptide 8 is also from the C-terminal region, containing one phosphorylated site, Ser-418. The vimentin in vivo phosphorylation sites that were identified during the course of this study are presented in Fig. 5 (newly identified in vivo phosphorylation sites are indicated with an asterisk).

Site-directed mutagenesis of two major PKA sites

Among the identified vimentin phosphorylation sites, two of the major sites (Ser-38, Ser-72) are PKA sites. To assess the role of these two phosphorylation sites in regulating vimentin IF assembly dynamics, we constructed a mutant version of myc-tagged human vimentin cDNA in which codons for these serine residues were substituted by those coding for alanine (S38:A/S72:A). Comparison of 2D tryptic phosphopeptide maps generated from equal amounts of either wild-type (Fig. 6A) or the S38:A/S72:A mutated vimentin (Fig. 6B) following in vitro phosphorylation with PKA, indicates a near complete loss of phosphorylation of the peptide containing Ser-38 (peptide 1), and a reduction in the level of that seen on the peptide containing Ser-72 (peptide 2). The residual phosphorylation on peptide 2 is likely to stem from phosphorylation of Ser-71, which has been shown to be a minor site for PKA (Geisler et al., 1989). Peptide 5 also showed a marked decrease in phosphorylation. This difference is intriguing, as it suggests that phosphorylation of Ser-38 and Ser-72 renders vimentin more susceptible to phosphorylation

Table 2. Suggested sequences for the phosphopeptides on the tryptic peptide maps

Peptide number on Fig. 3	Peptide number on Fig. 4 and Table 1	Manual Edman degradation: % label released on cycle number	Total number of cycles	Suggested sequence
1	6	3 (60%), 6 (30%), D (< 10%)	6	TYpSLGpSAL
2	3	3 (70%), 4 (20%), D (<10%)	6	LRpSpSMPGVR
3	3	3 (50%), 4 (30%), D (<10%)	6	LRpSpSMPGVR
4	7	6 (30%), D (>60%)	14	ETNLEpSLPLVDTHSK
5	1,2	1 (30%), 3 (30%), 5 (<10%), 6 (10%), D (<10%)	6	pSVpSSpSpSYR
6	1,2	5 (60%), 6 (30%), D (<10%)	6	SVSSpSpSYR
7	1,2	6 (70%), D (<10%)	6	SVSSSpSYR
8	5	6 (90%), D (<10%)	6	SLYSSpSPGGAYVTR
9	4	No release, D(>90%)	6	DGQVINEpTpSQHHDDLE

Manual Edman degradation was carried out on the phosphopeptides eluted from the TLC plates used for peptide mapping; D, disc. The results indicate the cycle when release of the label was observed. The suggested sequence for the peptide is partly based on the available sequence information and partly based on the knowledge of migration characteristics of previously isolated known phosphopeptides. The phosphorylation sites of peptide 4 to Thr-457 and Ser-458 were assigned based on Chou et al. (Chou et al., 1996).

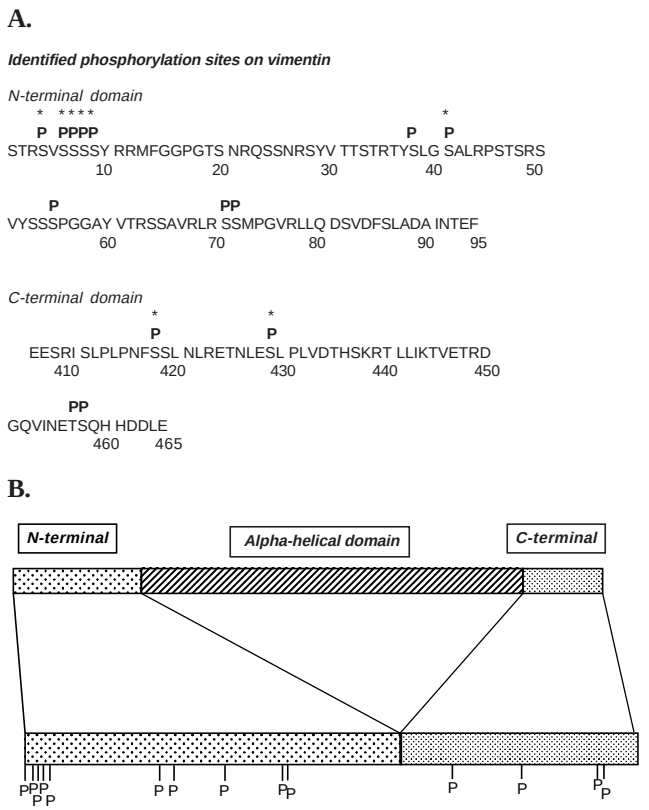

Fig. 5. Identified in vivo phosphorylation sites on vimentin. (A) A summary of all results obtained by phosphopeptide mapping, sequencing and manual Edman degradation. P, identified phosphorylation sites; *, sites that have not been previously described as in vivo phosphorylation sites. (B) The schematic figure shows the relative location of the phosphorylation sites in the N and C termini of vimentin.

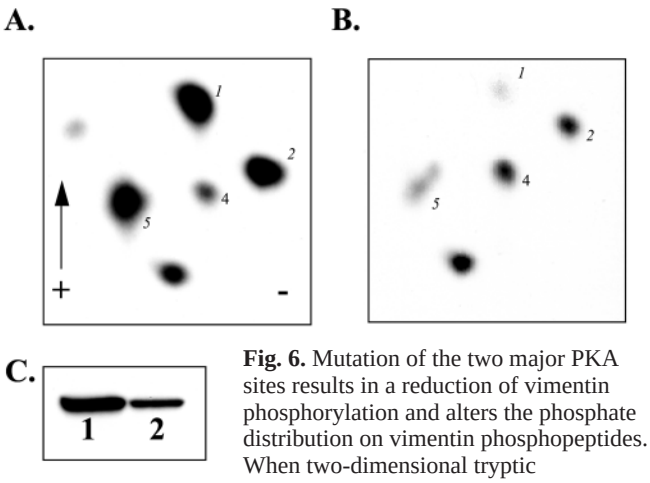

Fig. 6. Mutation of the two major PKA sites results in a reduction of vimentin phosphorylation and alters the phosphate distribution on vimentin phosphopeptides. When two-dimensional tryptic phosphopeptide mapping of PKA-phosphorylated (A) wild-type and (B) S38:A/S72:A vimentin was performed, peptide 1 showed negligible phosphorylation in the mutant vimentin, whereas peptide 2 showed reduced phosphorylation. Each map was loaded with peptides generated from 5 μg of ^{32}P-labeled vimentin. The direction of electrophoresis (+,-) and ascending chromatography (arrow) are indicated. (C) An overall reduction in ^{32}P incorporation as a result of the phosphate-site mutations could be seen when 7.5 μg of wild-type (lane 1) and S38:A/S72:A (lane 2) vimentin, respectively, were phosphorylated in vitro by PKA and subjected to one-dimensional SDS-PAGE followed by autoradiography.

of serines on peptide 5 (Ser-4, 6, 7, 8, and 9). Analysis of the specific PKA-induced phosphorylation of wild-type compared with S38:A/S72:A vimentin (7.5 μg of each loaded on 7.5% acrylamide SDS-PAGE) revealed a 50-65% reduction in the phosphorylation of S38:A/S72:A vimentin (Fig. 6C), with a reduction in the overall level of phosphorylation from 1.6-1.7 mole phosphate/mole for wild-type vimentin, to 0.6-0.8 mol phosphate/mole for S38:A/S72:A vimentin (results are ranges of values from five experiments).

Following in vitro phosphorylation, wild-type and S38:A/S72:A vimentin showed differences in the percentage of protein present in the pellet and supernatant fractions resulting from high-speed (200,000 ***g***) centrifugation of the kinase reaction mixtures. The amount of pelletable protein was inversely proportional to the amount of phosphate incorporated in the respective protein. With the wild-type protein, 30-40% was pelletable following in vitro PKA phosphorylation, while 80-85% of the PKA-phosphorylated S38:A/S72:A vimentin was pelletable (data not shown).

Phosphorylation by protein kinase A affects IF assembly in vivo

To assess the effects of phosphorylation on IF formation in vivo, wild-type, PKA-phosphorylated wild-type, and S38:A/S72:A myc-tagged vimentin were microinjected into BHK-21 cells. PKA was used because Ser-38 and Ser-S72 showed the largest increase in phosphorylation in BHK-21 cells in phosphatase inhibited cells. Microinjected protein was distinguished from endogenous BHK-21 cell vimentin using a monoclonal antibody directed against the myc-tag and a polyclonal anti-vimentin (Yang et al., 1985). Immediately following microinjection, non-phosphorylated wild-type vimentin formed small aggregates throughout the cytoplasm (data not shown). Within 10 minutes post-injection, the protein began to form short, filamentous rods (Fig. 7A, a) that elongated in close association with the endogenous vimentin IF network. The tagged protein was fully incorporated into the endogenous IF network within 30 minutes post-injection (Fig. 7A, b-c). When PKA-phosphorylated, wild-type vimentin (see Materials and Methods) was microinjected, a clear difference could be seen. After 10 minutes, only a diffuse fluorescence pattern was seen in the cytoplasm of microinjected cells (Fig. 7A, d). After 30 minutes, short filamentous rods were visible (Fig. 7A, e), but extended networks of IF were not seen with anti-myc until 3 hours after injection (Fig. 7A, f). The S38:A/S72:A mutated vimentin did not display any marked difference in the assembly kinetics, when compared to the kinetics of wild-type vimentin. After 3 hours, all three injected forms of vimentin were fully assembled, as indicated by the co-localization with the endogenous vimentin in analysis of double-label immunofluorescence using a polyclonal antibody specific for the endogenous vimentin (7B, a, b, and c). The images show the behavior of the S38:A/S72:A mutant vimentin but similar results were obtained with all three injected proteins. Taken together, this analysis shows that phosphorylation has a significant impact on the filament

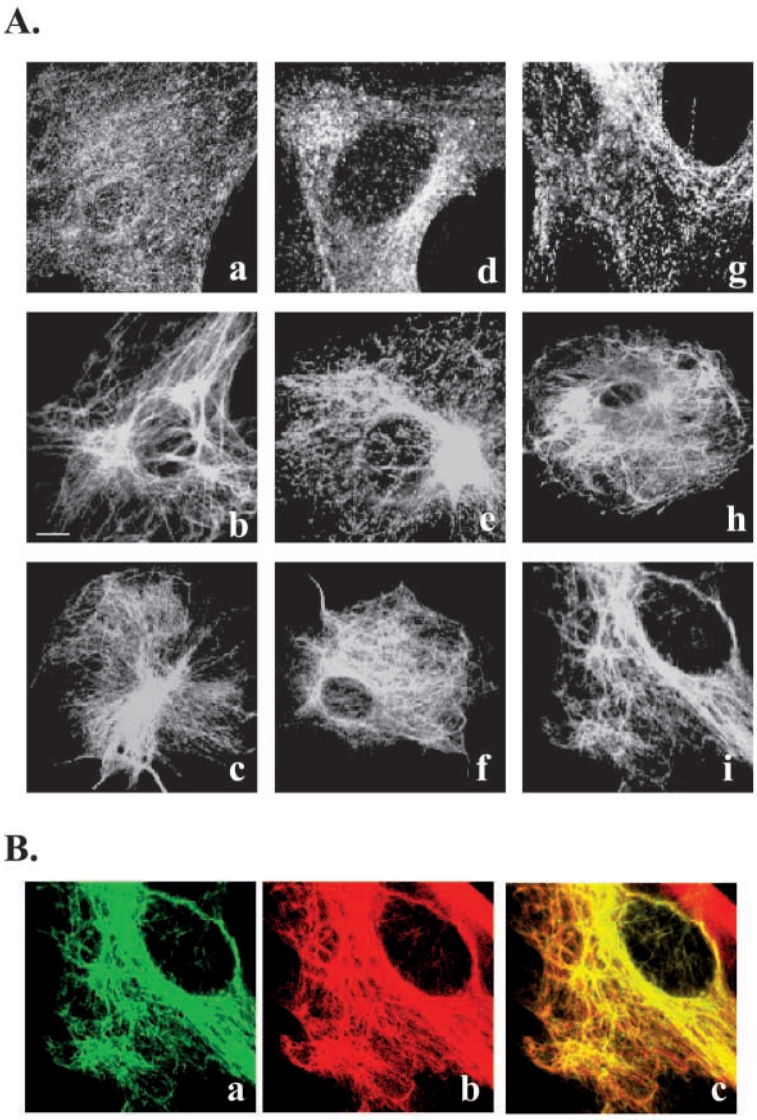

Fig. 7. Presence of phosphate groups on Ser-38 and Ser-72 affect filament forming ability following microinjection into BHK-21 fibroblasts. (A) Wild-type (a-c), PKA-phosphorylated wild-type supernatant fraction (d-f), and S38:A/S72:A (g-i) myc-tagged vimentin were microinjected at a concentration of 1 mg/ml into BHK-21 fibroblasts. At 10 minutes (a, d, g), 30 minutes (b, e, h) and 3 hours (c, f, i) post-injection, cells were fixed with methanol and indirect immunofluorescence was performed using a monoclonal antibody directed against the myc-tag to trace the microinjected protein. Filament formation by the injected protein was assessed, and confocal micrographs were obtained, demonstrating the degree of filament formation observed for the majority of cells at a given time point. (B) Co-localization of the injected protein with the endogenous BHK-21 IF network was determined at 3 hours post-injection by double-label immunofluorescence using a polyclonal antibody specific for the endogenous vimentin (a, b, c). The images show the behavior of the S38:A/S72:A mutant pelletable protein but similar results were obtained with all three injected proteins.

assembly, but that the absence of two critical phosphorylation sites does not affect the assembly to any greater extent.

Discussion

It is well established that IFs are highly dynamic structures, the constituent proteins of which undergo active exchange between a major compartment of assembled IF polymers and a very small fraction of disassembled IF subunits. In order to achieve these dynamic properties, IF proteins require an active support mechanism that maintains the exchange of subunits between the assembled and disassembled protein fractions. Reversible phosphorylation is a mechanism that could plausibly maintain this kind of exchange. Our results, obtained both by inhibition of dephosphorylation in vivo and by studying the in vivo assembly of phosphorylated and unphosphorylated forms of wild-type versus partially phosphorylation-deficient vimentin, indicate that both the equilibrium between vimentin polymers and depolymerized subunits and the turnover of subunit exchange are regulated by kinase-phosphatase equilibria. This regulation is based upon reversible phosphorylation of a number of phosphorylation sites located mainly in the N-terminal region of vimentin.

Protein phosphatase-mediated regulation of vimentin polymers

In accordance with previous studies (Eriksson et al., 1992a; Toivola et al., 1997), we demonstrate here that the integrity of IF polymers in vivo is dependent upon constitutive protein phosphatase activities, as the present results show that PP1 and PP2A inhibition results in rapid elevation of vimentin phosphorylation, with subsequent disassembly of the vimentin IFs. The vimentin released from the insoluble polymers can be divided into two protein pools, one consisting of fragmented filaments that are pelletable at high centrifugal forces, and one pool consisting of truly soluble subunits that are not pelletable. From our results, it appears that the elevated phosphorylation first induces a net fragmentation of the polymers and, when the phosphorylation is more markedly elevated, then induces a net release of soluble subunits. The specific ^{32}P labeling of two pelletable protein fractions was approximately at the same level, but the soluble pool had a 1.7-fold higher specific labeling, than the filament fractions. This indicates that the disassembly is driven by a net elevation in phosphorylation, with some selectivity for soluble subunits. Inversely, it could indicate that in the normal situation (in the absence of PP inhibitors), vimentin-directed PPs show preference for soluble subunits, which would explain why their presence is so scarce. The relative distribution of phosphate between soluble and pelletable fractions is to some extent different from that observed with keratin 8 and 18. While, vimentin is incorporated in all fractions (with some preference for soluble subunits), keratin 8/18 is incorporated predominantly in the solubilized subunits (Liao and Omary, 1996; Toivola et al., 1997).

The size of the disassembled vimentin subunits is of interest, as a knowledge of their composition could help elucidate how the exchange between polymers and the soluble pool of protein

occurs. Our results demonstrated that phosphorylation releases the same oligomeric peptide composition both in vitro and in vivo; tetrameric oligomers were released both by PKA phosphorylation in vitro and by inhibition of dephosphorylation in vivo. Previous in vitro studies have indicated that IF subunits usually occur in the tetrameric form (Downing, 1996; Foisner et al., 1991; Ip et al., 1985; Meng et al., 1996). In agreement with the in vitro results, it has been suggested that the minute soluble fraction of IF protein in vivo could be tetrameric in nature (Soellner et al., 1985). However, it has never been shown that phosphorylation would drive disassembly into the tetramer form. Our present results, showing that phosphorylation induces disassembly into tetrameric subunits, could imply that the phosphorylation-driven subunit exchange between IF polymers and soluble subunits would take place in the form of a tetramer.

Phosphatase inhibition reveals constitutive phosphate turnover on interphase-specific phosphorylation sites

Phosphopeptide mapping of the in vivo labeled vimentin shows that there is a large number of phosphorylation sites that undergo active turnover. As most of the phosphopeptides showing elevated phosphorylation in the presence of cl-A can also be discerned on the maps from control cells, we assume that the elevated phosphorylation is a true reflection of phosphate turnover and is not induced by phosphatase inhibitor-induced activation of kinases. In other words, although these sites have very low steady-state phosphate stoichiometry, they are still being actively phosphorylated, but then immediately also dephosphorylated.

The in vivo phosphopeptide maps were tested against a number of putative IF kinases, of which only PKA and PKC-generated phosphopeptides showed obvious matches with the phosphopeptides generated from in vivo ^{32}P-labeled vimentin isolated from interphase cells. Surprisingly, CaM kinase II did not show any obvious matches with the interphase phosphopeptides. In previous studies, CaM kinase has been shown to both phosphorylate vimentin in vitro and in vivo (Ogawara et al., 1995; Yano et al., 1994; Yano et al., 1991). As the generated CaM kinase-specific sites could not be observed in this study, these sites do not seem to belong to the sites that display active turnover, but are rather restricted to specific functions under certain physiological conditions and and/or in specific cell types.

Determining the in vivo phosphorylation sites by protein phosphatase inhibition

Ser-38 and Ser-72 were important phosphorylation targets in vivo and, as previously reported, these sites were phosphorylated by PKA in vitro. Interestingly, these sites have also been reported as targets for RhoA-binding kinase α (Goto et al., 1998; Sin et al., 1998). Apart from these N-terminal sites, there was a cluster of phosphorylated serines at the far N-terminus that showed a complex pattern of phosphorylation. On this Ser-cluster, there was a large number of different possible phospho-serine combinations present in vivo. While previous studies have indicated that Ser-6, Ser-8 and Ser-9 can be phosphorylated in vitro by PKC (Inagaki et al., 1997), Ser-4 and Ser-7 have not been reported to be phosphorylation targets. Apart from these sites, our study revealed a number of C-terminal sites as being actively phosphorylated. Of all these sites, Thr-457 and Ser-458 have been reported as specific mitotic sites in vivo, phosphorylated by the p37 vimentin kinase (Chou et al., 1996). Based on our current results, it appears that these sites are not phosphorylated entirely during mitosis but, at least to some extent, also in interphase. The observed Ser-418 and Ser-436 have never been reported as phosphorylation sites. The identity of the kinases phosphorylating these sites is not known and no putative kinases can be suggested, as the sequences surrounding these sites did not resemble any obvious kinase consensus sites. Curiously, the previously reported in vivo sites for PKC, Ser-33 and Ser-50, did not show up in this analysis at all (Takai et al., 1996), which could be due to cell-specific phosphate turnover characteristics on different cell lines.

Ser-38 and Ser-72 as specific PKA sites on vimentin

Mutation of Ser-38 and Ser-72 reduced the overall level of PKA-mediated phosphorylation on vimentin in vitro by 50-60%. The mutations did not result in a complete loss of phosphorylation on the tryptic phosphopeptides containing these sites, showing that in addition to the two ideal PKA consensus sites on these peptides (Ser-38: RXXS and Ser-72: RXS), other less typical sites on these two tryptic peptides are also phosphorylated by PKA.

Mutation of Ser-38 and Ser-72 had a marked effect on the PKA-mediated vimentin disassembly. While the bulk (70-80% of the total) of wild-type vimentin was disassembled into the soluble tetrameric form following in vitro phosphorylation with PKA, only a small disassembled pool (15-20% of total) resulted from the same treatment of S38:A/S72:A vimentin. This result is in line with previous studies showing that phosphorylation with PKA leads to an increased solubility of IF proteins (Inagaki et al., 1988; Inagaki et al., 1990; Yano et al., 1991), but also confirms that of all PKA sites, these two in particular are important in determining the assembly state of vimentin. The first in vivo study of PKA-mediated phosphorylation on vimentin structure was that by Lamb et al. (Lamb et al., 1989), showing marked effects on the organization of vimentin. Our present results corroborate these and later results, indicating the PKA-targeted phosphorylation sites, Ser-38 and Ser-72, are of major importance in maintaining and regulating vimentin structure.

The role of Ser-38 and Ser-72 in regulating the in vivo vimentin IF assembly dynamics

The microinjected bacterially expressed vimentin incorporated simultaneously at several places throughout the cytoplasm, forming a complete vimentin network in as little as 30 minutes following microinjection. This pattern of filament formation is quite similar to that previously described for de novo expression of transfected chicken vimentin in BALB/c 3T3 fibroblasts (Ngai et al., 1990), but differs from the pattern of filament formation previously reported for bovine lens vimentin. The latter incorporates in a very distinct pattern from the nuclear region outward and takes approximately 4 hours to form a complete IF network (Vikstrom et al., 1989; Vikstrom et al., 1991). The difference in the pattern of filament formation

following microinjection of these two different types of vimentin may be explained by the fact that these proteins are likely to be significantly different in their states of post-translational modification. Bacterial expression of human vimentin cDNA results in production of completely non-modified, 'virgin' protein. In contrast, it is to be expected that bovine lens vimentin would be highly post-translationally modified, because of the nature of the tissue from which it is derived (Vikstrom et al., 1991). Thus, this protein may have to be altered in some way before it can successfully form filaments in vivo. Our results support the assumption of a delay in incorporation of post-translationally modified vimentin, as a marked delay in filament formation could be induced by phosphorylation of vimentin with PKA preceding its microinjection into BHK-21 cells. If filament integrity in vivo is maintained by a balance of kinase and phosphatase activities as has been suggested (Eriksson et al., 1992a; Toivola et al., 1997), then it makes sense that it would take longer for the more phosphorylated, soluble supernatant fraction of vimentin to form filaments following injection, as phosphatase action may be required to achieve assembly competence. However, the absence of two major phosphorylation sites, Ser-38 and Ser-72, did not have a major effect on filament assembly, indicating that in regulating assembly equilibria, the role of phosphorylation is primarily to drive disassembly.

Possible roles of a continuous phosphate turnover

Our study identified a number of in vivo phosphorylation sites that are actively regulated. Our results indicate that overall phosphorylation of the whole vimentin pool on these sites increases the off-rate and, thereby, drives disassembly of polymers. However, dephosphorylation increases the on-rate, thereby driving the assembly of polymers. The complexity of the observed in vivo phosphorylation is striking, involving a large number of sites and even a high number of combinations of phosphorylated versus non-phosphorylated serines on adjacent sites. This complex phosphorylation pattern and phosphorylation of individual sites may reflect the fact that specific sites may have rather specific roles. Under these experimental conditions, some of the sites showed preferred phosphorylation, but it is likely that the relative importance of the respective sites vary significantly depending on the state of the cell. This presumption is well supported by the remarkable difference in the relative phosphate incorporation on interphase compared with mitotic sites.

Why is there a need for such an active phosphate turnover and dynamic regulation? In part, the answer is obvious: although IFs appear to have a definite shape and structure, in the live cells they are continuously restructured (Prahlad et al., 1998; Yoon et al., 1998). To restructure a complex network of proteins requires an active exchange of subunits for the remodeling to take place in a timely manner. As the nature of IF polymers is significantly different from those of actin and tubulin polymers, not allowing for the same type of dynamics as observed in these protein polymers, a mechanism involving post-translational modification needs to be involved. The active remodeling and subunit exchange may also have purposes other than mere restructuring of the IF networks. With respect to the phosphate turnover on Ser-38 and Ser-72 in particular, an interesting study raised the possibility that vimentin phosphorylation by RhoA-binding kinase α is likely to participate in regulating the targeting and sequestration of the kinase (Sin et al., 1998). Inactive kinase is largely found associated with vimentin IFs. When the small pool of free RhoA-binding kinase α is activated, it phosphorylates Ser-38 and Ser-72 on vimentin, thereby leading to a release, activation and relocalization of the inactive kinase pool (Sin et al., 1998). In addition, the p21-activated kinase has also been shown to interact with Ser-38 and Ser-72 (Goto et al., 2002).

As a number of other kinases, including various PKC isoforms, cdc2, cdk5 and cyclic GMP-dependent protein kinase (MacMillan-Crow and Lincoln, 1994; Spudich et al., 1992; Wyatt et al., 1991), have been found associated with vimentin and other IFs (Dosemeci and Pant, 1992; Hollander and Bennett, 1992; Omary et al., 1992; Starr et al., 1996; Xiao and Monteiro, 1994), it is tempting to speculate that the phosphorylation sites present on the various parts of vimentin could be involved in similar types of sequestering or scaffolding processes, as that described above for RhoA-binding kinase α. It remains to be resolved whether, for example, the numerous putative PKC sites at the far end of the vimentin N terminus could be involved in this kind of autoregulatory sequestering and targeting functions.

We thank Howard Schulman (Stanford University School of Medicine) for the recombinant CaMKII. We are grateful to Helena Saarento for excellent technical assistance. This work was supported by the Academy of Finland and the Research Institute of the Åbo Akademi Foundation. T.H. was supported by the Turku Graduate School of Biomedical Sciences.

References

Aitken, A. (1996). 14-3-3 and its possible role in co-ordinating multiple signalling pathways. *Trends Cell Biol.* **6**, 341-347.

Almazan, G., Afar, D. E. and Bell, J. C. (1993). Phosphorylation and disruption of intermediate filament proteins in oligodendrocyte precursor cultures treated with calyculin A. *J. Neurosci. Res.* **36**, 163-172.

Ando, S., Tokui, T., Yamauchi, T., Sugiura, H., Tanabe, K. and Inagaki, M. (1991). Evidence that Ser-82 is a unique phosphorylation site on vimentin for Ca2(+)-calmodulin-dependent protein kinase II. *Biochem. Biophys. Res. Commun.* **175**, 955-962.

Ando, S., Tokui, T., Yano, T. and Inagaki, M. (1996). Keratin 8 phosphorylation in vitro by cAMP-dependent protein kinase occurs within the amino- and carboxyl-terminal end domains. *Biochem. Biophys. Res. Commun.* **221**, 67-71.

Caulin, C., Ware, C. F., Magin, T. M. and Oshima, R. G. (2000). Keratin-dependent, epithelial resistance to tumor necrosis factor-induced apoptosis. *J. Cell Biol.* **149**, 17-22.

Chou, Y. H., Bischoff, J. R., Beach, D. and Goldman, R. D. (1990). Intermediate filament reorganization during mitosis is mediated by p34cdc2 phosphorylation of vimentin. *Cell* **62**, 1063-1071.

Chou, Y. H., Ngai, K. L. and Goldman, R. (1991). The regulation of intermediate filament reorganization in mitosis. p34cdc2 phosphorylates vimentin at a unique N-terminal site. *J. Biol. Chem.* **266**, 7325-7328.

Chou, Y. H., Opal, P., Quinlan, R. A. and Goldman, R. D. (1996). The relative roles of specific N- and C-terminal phosphorylation sites in the disassembly of intermediate filament in mitotic BHK-21 cells. *J. Cell Sci.* **109**, 817-826.

Chou, Y. H., Skalli, O. and Goldman, R. D. (1997). Intermediate filaments and cytoplasmic networking: new connections and more functions. *Curr. Opin. Cell Biol.* **9**, 49-53.

Dosemeci, A. and Pant, H. C. (1992). Association of cyclic-AMP-dependent protein kinase with neurofilaments. *Biochem. J.* **282**, 477-481.

Downing, D. T. (1996). Molecular modeling of vimentin filament assembly. *Proteins* **26**, 472-478.

Eriksson, J. E., Brautigan, D. L., Vallee, R., Olmsted, J., Fujiki, H. and Goldman, R. D. (1992a). Cytoskeletal integrity in interphase cells requires protein phosphatase activity. *Proc. Natl. Acad. Sci. USA* **89**, 11093-11097.

Eriksson, J. E., Opal, P. and Goldman, R. D. (1992b). Intermediate filament dynamics. *Curr. Opin. Cell Biol.* **4**, 99-104.

Eriksson, J. E., Toivola, D. M., Sahlgren, C., Mikhailov, A. and Harmala-Brasken, A. S. (1998). Strategies to assess phosphoprotein phosphatase and protein kinase-mediated regulation of the cytoskeleton. *Methods Enzymol.* **298**, 542-569.

Feng, L., Zhou, X., Liao, J. and Omary, M. B. (1999). Pervanadate-mediated tyrosine phosphorylation of keratins 8 and 19 via a p38 mitogen-activated protein kinase-dependent pathway. *J. Cell Sci.* **112**, 2081-2090.

Foisner, R., Traub, P. and Wiche, G. (1991). Protein kinase A- and protein kinase C-regulated interaction of plectin with lamin B and vimentin. *Proc. Natl. Acad. Sci. USA* **88**, 3812-3816.

Fuchs, E. and Cleveland, D. W. (1998). A structural scaffolding of intermediate filaments in health and disease. *Science* **279**, 514-519.

Geisler, N., Hatzfeld, M. and Weber, K. (1989). Phosphorylation in vitro of vimentin by protein kinases A and C is restricted to the head domain. Identification of the phosphoserine sites and their influence on filament formation. *Eur. J. Biochem.* **183**, 441-447.

Giasson, B. I. and Mushynski, W. E. (1996). Aberrant stress-induced phosphorylation of perikaryal neurofilaments. *J. Biol. Chem.* **271**, 30404-30409.

Goldman, R., Goldman, A., Green, K., Jones, J., Lieska, N. and Yang, H. Y. (1985). Intermediate filaments: possible functions as cytoskeletal connecting links between the nucleus and the cell surface. *Ann. NY Acad. Sci*. **455**, 1-17.

Goldman, R. D., Chou, Y. H., Prahlad, V. and Yoon, M. (1999). Intermediate filaments: dynamic processes regulating their assembly, motility, and interactions with other cytoskeletal systems. *FASEB J.* **13 Suppl. 2**, S261-2615.

Goldman, R. D., Goldman, A. E., Green, K. J., Jones, J. C., Jones, S. M. and Yang, H. Y. (1986). Intermediate filament networks: organization and possible functions of a diverse group of cytoskeletal elements. *J. Cell Sci. Supplement* **5**, 69-97.

Goto, H., Kosako, H., Tanabe, K., Yanagida, M., Sakurai, M., Amano, M., Kaibuchi, K. and Inagaki, M. (1998). Phosphorylation of vimentin by Rho-associated kinase at a unique amino-terminal site that is specifically phosphorylated during cytokinesis. *J. Biol. Chem.* **273**, 11728-11736.

Goto, H., Tanabe, K., Manser, E., Lim, L., Yasui, Y., and Inagaki, M. (2002). Phosphorylation and reorganization of vimentin by p21-activated kinase (PAK). *Genes Cells* **7**, 91-97.

He, T., Stepulak, A., Holmstrom, T. H., Omary, M. B. and Eriksson, J. E. (2002). The intermediate filament protein keratin 8 is a novel cytoplasmic substrate for c-Jun N-terminal kinase. *J. Biol. Chem.* **277**, 10767-10774.

Hollander, B. A. and Bennett, G. S. (1992). Characterization of a neurofilament-associated kinase that phosphorylates the middle molecular mass component of chicken neurofilaments. *Brain Res.* **599**, 237-245.

Holmberg, C. I., Hietakangas, V., Mikhailov, A., Rantanen, J. O., Kallio, M., Meinander, A., Hellman, J., Morrice, N., MacKintosh, C., Morimoto, R. I., Eriksson, J. E. and Sistonen, L. (2001). Phosphorylation of serine 230 promotes the inducible transcriptional activity of heat shock factor 1. *EMBO J.* **20**, 3800-3810.

Inada, H., Izawa, I., Nishizawa, M., Fujita, E., Kiyono, T., Takashi, T., Momoi, T. and Inagaki, M. (2001). Keratin attenuates tumor necrosis factor-induced cytotoxicity through association with TRADD. *J. Cell Biol.* **155**, 415-426.

Inagaki, M., Gonda, Y., Matsuyama, M., Nishizawa, K., Nishi, Y. and Sato, C. (1988). Intermediate filament reconstitution in vitro. The role of phosphorylation on the assembly-disassembly of desmin. *J. Biol. Chem.* **263**, 5970-5978.

Inagaki, M., Gonda, Y., Nishizawa, K., Kitamura, S., Sato, C., Ando, S., Tanabe, K., Kikuchi, K., Tsuiki, S. and Nishi, Y. (1990). Phosphorylation sites linked to glial filament disassembly in vitro locate in a non-alpha-helical head domain. *J. Biol. Chem.* **265**, 4722-4729.

Inagaki, M., Inagaki, N., Takahashi, T. and Takai, Y. (1997). Phosphorylation-dependent control of structures of intermediate filaments: a novel approach using site- and phosphorylation state-specific antibodies. *J. Biochem.* **121**, 407-414.

Inagaki, M., Matsuoka, Y., Tsujimura, K., Ando, S., Tokui, T., Takahashi, T., and Inagaki, N. (1996). Dynamic property of intermediate filaments: regulation by phosphorylation. *BioEssay* **18**, 481-487.

Ip, W., Hartzer, M. K., Pang, Y. Y. and Robson, R. M. (1985). Assembly of vimentin in vitro and its implications concerning the structure of intermediate filaments. *J. Mol. Biol.* **183**, 365-375.

Janosch, P., Kieser, A., Eulitz, M., Lovric, J., Sauer, G., Reichert, M., Gounari, F., Buscher, D., Baccarini, M. Mischak, H. et al. (2000). The Raf-1 kinase associates with vimentin kinases and regulates the structure of vimentin filaments. *FASEB J.* **14**, 2008-2021.

Ku, N. O., Liao, J., Chou, C. F. and Omary, M. B. (1996). Implications of intermediate filament protein phosphorylation. *Cancer Metastasis Rev.* **15**, 429-444.

Ku, N. O., Liao, J. and Omary, M. B. (1998). Phosphorylation of human keratin 18 serine 33 regulates binding to 14-3-3 proteins. *EMBO J.* **17**, 1892-1906.

Kunkel, T. A. (1985). Rapid and efficient site-specific mutagenesis without phenotypic selection. *Proc. Natl. Acad. Sci. USA* **82**, 488-492.

Lamb, N. J., Fernandez, A. and Welch, W. J. (1989). Modulation of vimentin containing intermediate filament distribution and phosphorylation in living cells by cAMP-dependent protein kinase. *J. Cell Biol.* **108**, 2409-2422.

Laemmli, U. K. (1970). Cleavage of structural proteins during the assembly of the head of bacteriophage T4. *Nature* **227**, 680-685.

Lee, W. C., Yu, J. S., Yang, S. D. and Lai, Y. K. (1992). Reversible hyperphosphorylation and reorganization of vimentin intermediate filaments by okadaic acid in 9L rat brain tumor cells. *J. Cell Biochem.* **49**, 378-393.

Li, Y. M., Mackintosh, C. and Casida, J. E. (1993). Protein phosphatase 2A and its [3H]cantharidin/[3H]endothall thioanhydride binding site. Inhibitor specificity of cantharidin and ATP analogues. *Biochem. Pharmacol.* **46**, 1435-1443.

Liao, J. and Omary, M. B. (1996). 14-3-3 proteins associate with phosphorylated simple epithelial keratins during cell cycle progression and act as a solubility cofactor. *J. Cell Biol.* **133**, 345-357.

MacMillan-Crow, L. A. and Lincoln, T. M. (1994). High-affinity binding and localization of the cyclic GMP-dependent protein kinase with the intermediate filament protein vimentin. *Biochemistry* **33**, 8035-8043.

Meng, J. J., Khan, S. and Ip, W. (1996). Intermediate filament protein domain interactions as revealed by two-hybrid screens. *J. Biol. Chem.* **271**, 1599-1604.

Miller, R. K., Vikstrom, K. and Goldman, R. D. (1991). Keratin incorporation into intermediate filament networks is a rapid process. *J. Cell Biol.* **113**, 843-855.

Ngai, J., Coleman, T. R. and Lazarides, E. (1990). Localization of newly synthesized vimentin subunits reveals a novel mechanism of intermediate filament assembly. *Cell* **60**, 415-427.

Ogawara, M., Inagaki, N., Tsujimura, K., Takai, Y., Sekimata, M., Ha, M. H., Imajoh-Ohmi, S., Hirai, S., Ohno, S., Sugiura, H. et al. (1995). Differential targeting of protein kinase C and CaM kinase II signalings to vimentin. *J. Cell Biol.* **131**, 1055-1066.

Ohta, T., Nishiwaki, R., Yatsunami, J., Komori, A., Suganuma, M. and Fujiki, H. (1992). Hyperphosphorylation of cytokeratins 8 and 18 by microcystin-LR, a new liver tumor promoter, in primary cultured rat hepatocytes. *Carcinogenesis* **13**, 2443-2447.

Omary, M. B., Baxter, G. T., Chou, C. F., Riopel, C. L., Lin, W. Y. and Strulovici, B. (1992). PKC epsilon-related kinase associates with and phosphorylates cytokeratin 8 and 18. *J. Cell Biol.* **117**, 583-593.

Omary, M. B. and Ku, N. O. (1997). Intermediate filament proteins of the liver: emerging disease association and functions. *Hepatology* **25**, 1043-1048.

Prahlad, V., Yoon, M., Moir, R. D., Vale, R. D. and Goldman, R. D. (1998). Rapid movements of vimentin on microtubule tracks: kinesin-dependent assembly of intermediate filament networks. *J. Cell Biol.* **143**, 159-170.

Sin, W. C., Chen, X. Q., Leung, T. and Lim, L. (1998). RhoA-binding kinase alpha translocation is facilitated by the collapse of the vimentin intermediate filament network. *Mol. Cell. Biol.* **18**, 6325-6339.

Sistonen, L., Sarge, K. D. and Morimoto, R. I. (1994). Human heat shock factors 1 and 2 are differentially activated and can synergistically induce hsp70 gene transcription. *Mol. Cell. Biol.* **14**, 2087-2099.

Skalli, O., Chou, Y. H. and Goldman, R. D. (1992). Cell cycle-dependent changes in the organization of an intermediate filament-associated protein: correlation with phosphorylation by p34cdc2. *Proc. Natl. Acad. Sci. USA* **89**, 11959-11963.

Soellner, P., Quinlan, R. A. and Franke, W. W. (1985). Identification of a distinct soluble subunit of an intermediate filament protein: tetrameric vimentin from living cells. *Proc. Natl. Acad. Sci. USA* **82**, 7929-7933.

Spudich, A., Meyer, T. and Stryer, L. (1992). Association of the beta isoform of protein kinase C with vimentin filaments. *Cell. Motil. Cytoskel.* **22**, 250-256.

Starr, R., Hall, F. L. and Monteiro, M. J. (1996). A cdc2-like kinase distinct from cdk5 is associated with neurofilaments. *J. Cell Sci.* **109**, 1565-1573.

Takai, Y., Ogawara, M., Tomono, Y., Moritoh, C., Imajoh-Ohmi, S.,

Tsutsumi, O., Taketani, Y. and Inagaki, M. (1996). Mitosis-specific phosphorylation of vimentin by protein kinase C coupled with reorganization of intracellular membranes. *J. Cell Biol.* **133**, 141-149.

Toivola, D. M., Goldman, R. D., Garrod, D. R. and Eriksson, J. E. (1997). Protein phosphatases maintain the organization and structural interactions of hepatic keratin intermediate filaments. *J. Cell Sci.* **110**, 23-33.

Tsujimura, K., Tanaka, J., Ando, S., Matsuoka, Y., Kusubata, M., Sugiura, H., Yamauchi, T. and Inagaki, M. (1994). Identification of phosphorylation sites on glial fibrillary acidic protein for cdc2 kinase and Ca(2+)-calmodulin-dependent protein kinase II. *J. Biochem.* **116**, 426-434.

Tzivion, G., Luo, Z. J. and Avruch, J. (2000). Calyculin A-induced vimentin phosphorylation sequesters 14-3-3 and displaces other 14-3-3 partners in vivo. *J. Biol. Chem.* **275**, 29772-29778.

Vikstrom, K. L., Borisy, G. G. and Goldman, R. D. (1989). Dynamic aspects of intermediate filament networks in BHK-21 cells. *Proc. Natl. Acad. Sci. USA* **86**, 549-553.

Vikstrom, K. L., Miller, R. K. and Goldman, R. D. (1991). Analyzing dynamic properties of intermediate filaments. *Methods Enzymol.* **196**, 506-525.

Wyatt, T. A., Lincoln, T. M. and Pryzwansky, K. B. (1991). Vimentin is transiently co-localized with and phosphorylated by cyclic GMP-dependent protein kinase in formyl-peptide-stimulated neutrophils. *J. Biol. Chem.* **266**, 21274-21280.

Xiao, J. and Monteiro, M. J. (1994). Identification and characterization of a novel (115 kDa) neurofilament-asociated kinase. *J. Neurosci.* **14**, 1820-1833.

Yang, H. Y., Lieska, N., Goldman, A. E. and Goldman, R. D. (1985). A 300,000-mol-wt intermediate filament-associated protein in baby hamster kidney (BHK-21) cells. *J. Cell Biol.* **100**, 620-631.

Yano, S., Fukunaga, K., Ushio, Y. and Miyamoto, E. (1994). Activation of Ca2+/calmodulin-dependent protein kinase II and phosphorylation of intermediate filament proteins by stimulation of glutamate receptors in cultured rat cortical astrocytes. *J. Biol. Chem.* **269**, 5428-5439.

Yano, T., Tokui, T., Nishi, Y., Nishizawa, K., Shibata, M., Kikuchi, K., Tsuiki, S., Yamauchi, T. and Inagaki, M. (1991). Phosphorylation of keratin intermediate filaments by protein kinase C, by calmodulin-dependent protein kinase and by cAMP-dependent protein kinase. *Eur. J. Biochem.* **197**, 281-290.

Yoon, M., Moir, R. D., Prahlad, V. and Goldman, R. D. (1998). Motile properties of vimentin intermediate filament networks in living cells. *J. Cell Biol.* **143**, 147-157.